

Electron transport, ionization, and attachment coefficients in C_2F_4 and C_2F_4/Ar mixtures

A. N. Goyette

Electricity Division, National Institute of Standards and Technology, Gaithersburg, Maryland 20899-8113

J. de Urquijo

Centro de Ciencias Físicas, Universidad Nacional Autónoma de México, P.O. Box 48-3, 62251 Cuernavaca, Mor. México

Yicheng Wang, L. G. Christophorou, and J. K. Olthoff

Electricity Division, National Institute of Standards and Technology, Gaithersburg, Maryland 20899-8113

(Received 28 December 2000; accepted 8 March 2001)

Measurements of electron transport, effective ionization, and attachment coefficients are reported for C_2F_4 . In addition, measurements of the electron drift velocity and the effective ionization coefficient as a function of the density-reduced electric field E/N are reported for mixtures of C_2F_4 with Ar. The measured effective ionization coefficients in C_2F_4/Ar mixtures indicates a contribution to these coefficients from Penning ionization in dilute C_2F_4/Ar mixtures. The rate constant for electron attachment to C_2F_4 as well as the product of the longitudinal electron diffusion coefficient and the gas number density ND_L in mixtures of C_2F_4 with Ar as functions of E/N are also reported.

© 2001 American Institute of Physics. [DOI: 10.1063/1.1368385]

I. INTRODUCTION

In the use of perfluorocyclobutane ($c-C_4F_8$) as a plasma processing gas for silicon dioxide etching (e.g., see Refs. 1–5), perfluoroethylene (C_2F_4) is produced as a by-product of electron and photon impact on $c-C_4F_8$, and also as a product of thermal decomposition of $c-C_4F_8$ (e.g., Refs. 6–12). Consequently, dissociative processes can make C_2F_4 a significant gas constituent. Therefore, in order to model $c-C_4F_8$ plasmas, it is important to know the electron transport, ionization, and attachment coefficients of C_2F_4 so as to understand fully the chemical and physical processes occurring in the discharge. This knowledge may also be of relevance to gaseous dielectrics since C_2F_4 may be produced in SF_6 circuit breakers by vaporization of polytetrafluoroethylene insulators.^{13,14}

Measurements of electron transport, ionization, and attachment coefficients are reported in this paper for pure C_2F_4 gas. In addition, measurements of the electron drift velocity and the effective ionization coefficient as functions of the density-reduced electric field E/N are reported for mixtures of C_2F_4 with Ar, which may be useful in efforts to obtain electron collision cross sections for C_2F_4 using Boltzmann codes. The effect of Penning ionization on the measured effective ionization coefficients in C_2F_4/Ar mixtures is also investigated. Additionally, the present paper reports measurements of the rate constant for electron attachment to C_2F_4 as a function of E/N . The electron attachment data are discussed in connection with the lowest negative ion states of C_2F_4 involving π^* and σ^* orbitals.

II. EXPERIMENT

The experimental work described in this paper has been conducted at the National Institute of Standards and Technology (NIST) in Gaithersburg, Maryland and at the Univer-

sidad Nacional Autónoma de México (UNAM). The independent measurements at the two laboratories complement and cross check each other. The NIST measurements best cover the low E/N region, and the UNAM measurements best cover the high E/N region.

The experimental method employed at NIST is the pulsed Townsend technique,¹⁵ and the experimental apparatus is the same as that used previously for similar measurements in CCl_2F_2 and CHF_3 .^{16,17} Electron swarms are photoelectrically produced at the cathode by a frequency-quadrupled Nd:YAG laser. A distance of 1.602 cm separates the two electrodes of the parallel plate drift arrangement. The laser beam enters the chamber through a sapphire window and is focused by a converging lens through a small hole in the center of the anode before striking the cathode. The induced signal is amplified and then digitized using a digital oscilloscope.

If the laser pulse duration is short compared to the drift time of the electrons and if electron impact ionization and electron attachment are the dominant electron and ion production processes, then the electron current can be described by¹⁸

$$i_e(t, D_L) = i_0 \exp[\bar{\alpha} w(t - t_0)] \frac{\text{erfc}(\xi)}{2} \quad (1)$$

with

$$\xi = \frac{(w + \bar{\alpha} D_L)(t - t_0) - d}{\sqrt{4 D_L (t - t_0)}}, \quad (2)$$

and $\text{erfc}(\xi) = 1 - \text{erf}(\xi)$ is the complementary error function; i_0 is the current due to the initial electrons; $\bar{\alpha} = \alpha - \eta$ is the effective ionization coefficient and α and η are the ionization and attachment coefficients, respectively; w is the electron drift velocity; D_L is the longitudinal electron diffusion coef-

ficient; d is the interelectrode gap; and t_0 is the time value corresponding to the beginning of the current waveform. Experimental electron current waveforms were fitted to Eq. (1) using a nonlinear least squares analysis with $\bar{\alpha}$, w , D_L , and i_0 as fitting parameters. For consistency, t_0 was taken to be the time at which the first derivative of the current waveform reached its maximum, and was held fixed during the fitting.

The experimental method employed at UNAM is also the pulsed Townsend technique, and the experimental apparatus is the same as used previously for similar measurements in CH₄ (Ref. 19) and CHF₃.²⁰ Electron swarms are photoelectrically produced at the cathode by a pulsed nitrogen laser ($\lambda=337$ nm, 1.4 mJ, 1 ns duration). A fixed gap spacing of 3 cm was set with an uncertainty of 0.1%. The laser beam enters the chamber through a quartz window and a laser copper mesh at the anode before striking the cathode. The displacement current across the gap is amplified in the external circuit by a 10^5 V/A transresistance amplifier, and registered by a digital oscilloscope. The overall bandwidth of the detection system was 40 MHz. A description of the analysis of the current waveform is given in Ref. 20.

All measurements were made at room temperature; ~ 298 K at NIST and between 297 K and 302 K at UNAM. The electron drift velocity measurements have an estimated uncertainty of $\pm 5\%$ for both sets of apparatus, and the uncertainty of the other measurements is estimated to be $\pm 10\%$.

The same C₂F₄ gas was used at the two laboratories. The C₂F₄ gas was "passivated" with D-limonene as supplied by ABCR GmbH & Co. KG.²¹ It has a stated purity of $>99\%$. Both the C₂F₄ and the research grade Ar used were further purified by freeze-pump-thaw cycles before use. D-limonene has a boiling point of ~ 450 K and therefore is expected to have negligible vapor pressure at room temperature.

III. RESULTS AND DISCUSSION

A. Electron drift velocity as a function of E/N , $w(E/N)$

Figure 1 shows the $w(E/N)$ for 100% C₂F₄ measured at NIST (closed points) and at UNAM (open points). The agreement between the measurements made independently at the two laboratories is good and the data complement each other in terms of the E/N range covered. The NIST data are the average of measurements made at pressures of 0.267 kPa, 0.666 kPa, and 1.333 kPa and the UNAM data are the averages of measurements made at 8 values of the gas pressure ranging from 0.066 kPa to 1.333 kPa. The variation of these measurements with pressure for a given value of E/N is within their stated uncertainty. The solid line in Fig. 1 is a least squares fit to the data of UNAM above 300×10^{-17} V cm², the data of both UNAM and NIST between 20×10^{-17} V cm² and 300×10^{-17} V cm², and the data of NIST below 20×10^{-17} V cm². Values from this line are listed in Table I.²²

Figure 2 shows $w(E/N)$ values for mixtures of C₂F₄ with Ar at relative C₂F₄ concentrations of 0.1%, 0.5%, 1%, 5%, and 10% (NIST measurements, closed points) and at 0.025%, 0.05%, 0.1%, 0.5%, 1%, and 5% (UNAM measure-

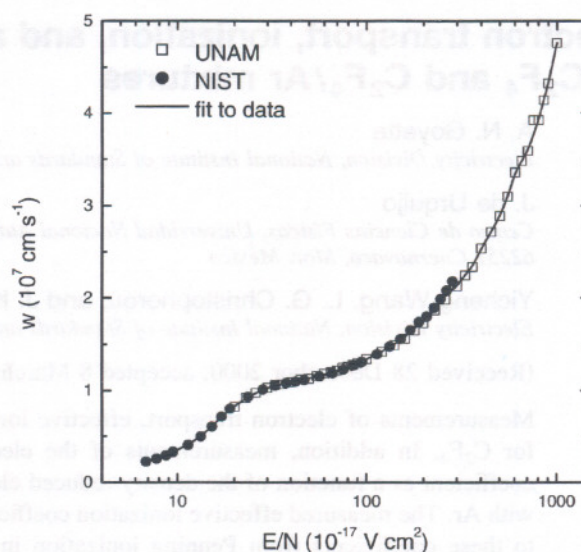


FIG. 1. Electron drift velocity, $w(E/N)$, for 100% C₂F₄. □, measurements at UNAM; ●, measurements at NIST; —, least squares average (see text).

ments, open points). Again the agreement between the two independent measurements is good. Also shown in Fig. 2 are $w(E/N)$ data for 100% Ar for comparison.²³ The lines in Fig. 2 for each mixture represent a least squares average of all data for that mixture. Values taken off the lines in Fig. 2 are also listed in Table I.

It is interesting to observe the distinct regions of negative differential conductivity exhibited by the data in Fig. 2. The values of E/N at which the drift velocity exhibits a local maximum, $(E/N)_{\max}$, vary linearly with the percentage of C₂F₄ in Ar for the compositions employed (Fig. 3). This behavior is similar to that observed earlier^{17,24} for mixtures of CHF₃ with Ar. A maximum in the drift velocity would indicate a minimum in the magnitude of the overall electron scattering cross section in a certain electron energy range. If the drift velocity maxima result from electrons being scattered by C₂F₄ into the energy region where the electron scattering cross section of Ar has a minimum [~ 0.23 eV (Ref. 25)], the values of $(E/N)_{\max}$ would represent the E/N value at which the average electron energy in the corresponding mixture is ~ 0.23 eV. As the percentage of C₂F₄ in Ar is increased, because C₂F₄ is more efficient in slowing down the electrons than Ar, the value of E/N for which the energy of the electrons lies in the region of the cross section minimum increases. This explains why $(E/N)_{\max}$ shifts to higher E/N values as the percentage of C₂F₄ in the mixture is increased.

B. Product of the longitudinal electron diffusion coefficient and the total gas number density as a function of E/N , $ND_L(E/N)$

Figure 4 shows the product of the longitudinal electron diffusion coefficient and the total gas number density, ND_L , as a function of E/N for mixtures of C₂F₄ with Ar. The values were obtained from fitting experimental waveforms to Eq. (1). At each mixture composition shown, ND_L goes

TABLE I. Values of the electron drift velocity, w , and effective ionization coefficient, $\bar{\alpha}/N$, in C_2F_4 as a function of E/N .

E/N (10^{-17} V cm 2)	w (10^6 cm s $^{-1}$)	$\bar{\alpha}/N$ (10^{-16} cm 2)
7.00	2.31	-0.298
8.00	2.65	-0.244
9.00	3.06	-0.197
10.0	3.51	-0.157
12.0	4.37	-0.110
14.0	5.41	-0.0832
16.0	6.56	-0.0586
18.0	7.54	-0.0415
20.0	8.27	-0.0332
23.0	9.12	-0.0274
26.0	9.71	-0.0229
30.0	10.3	-0.0207
35.0	10.7	-0.0213
40.0	10.9	-0.0169
45.0	11.1	-0.0138
50.0	11.3	-0.0132
60.0	11.7	-0.0120
70.0	12.1	-0.0111
80.0	12.5	-0.0101
90.0	12.9	-0.008 50
100	13.3	-0.006 37
120	14.2	-0.001 56
140	15.0	0.005 63
160	15.8	0.0153
180	16.7	0.0279
200	17.5	0.0422
230	18.8	0.0691
260	20.2	0.0998
300	21.3	0.149
350	23.1	0.226
400	25.4	0.306
450	27.2	0.396
500	28.9	0.498
600	33.6	0.678
700	35.9	0.887
800	39.2	1.070
900	43.2	...
1000	47.6	...

through a maximum which shifts to higher values of E/N and decreases in value with increasing percentage of C_2F_4 in Ar. These characteristics are again related to the lowering of the electron energies as the percentage of C_2F_4 in Ar is increased.

C. Density-reduced effective ionization coefficient as a function of E/N , $(\alpha - \eta)/N(E/N)$

1. $(\alpha - \eta)/N(E/N)$ for C_2F_4

Figure 5 shows the measured values of the density-reduced effective ionization coefficient $(\alpha - \eta)/N$ as a function of E/N for 100% C_2F_4 . The solid line shown in Fig. 5 is at least squares fit to the UNAM data above 300×10^{-17} V cm 2 , the UNAM and NIST data between 20×10^{-17} V cm 2 and 300×10^{-17} V cm 2 , and the NIST data below 20×10^{-17} V cm 2 . Values obtained from the fit are listed in Table I. The data in Fig. 5 show that the limiting value, $(E/N)_{lim}$, of E/N [value of E/N at which $(\alpha - \eta)/N \rightarrow 0$] for this gas is $\sim 130 \times 10^{-17}$ V cm 2 . This value is shown in Fig. 5 by the vertical arrow.

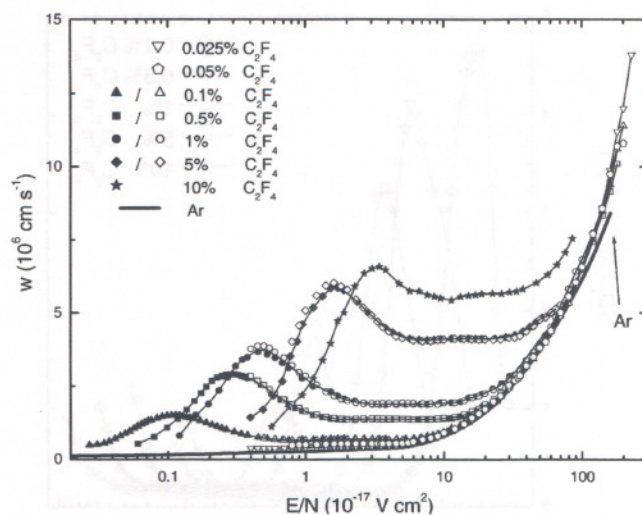


FIG. 2. Electron drift velocity, $w(E/N)$, in mixtures of C_2F_4 with Ar at concentrations (by number density) of 0.025%, 0.05%, 0.1%, 0.5%, 1%, 5%, and 10%. For comparison, the $w(E/N)$ for pure Ar are also plotted in the figure. The solid points are measurements made at NIST and the open points are measurements made at UNAM. The solid lines through the data for each mixture are least squares fits to all the data points.

The negative values of $(\alpha - \eta)/N$ at lower E/N can be attributed to attachment to C_2F_4 (see Sec. III D) or perhaps to a strongly attaching impurity.

2. $(\alpha - \eta)/N(E/N)$ for C_2F_4 /Ar gas mixtures

Figure 6 shows measurements of $(\alpha - \eta)/N$ for C_2F_4 /Ar gas mixtures, where N is taken to be the total gas number density of the mixture. These measurements were made in the usual way, that is, by subtracting from the measured current the positive ion current contribution as determined by the size of the current at long times (see discussion later in this section). Also shown in Fig. 6 for comparison are the value of $(\alpha - \eta)/N$ for 100% C_2F_4 (---) from Table I and the value of α/N for pure Ar (—). The solid line for Ar repre-

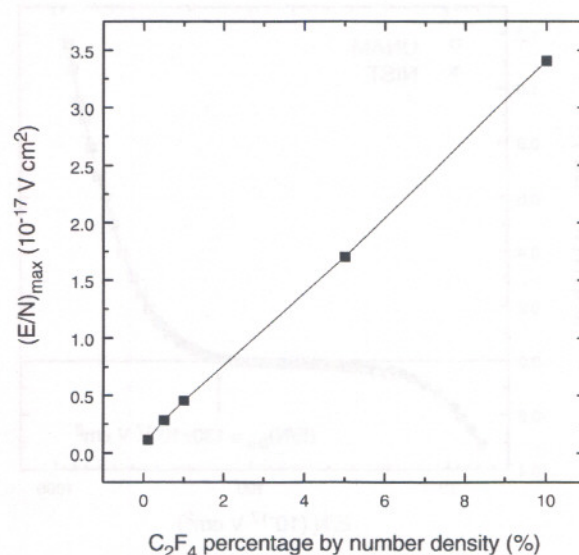


FIG. 3. Variation of the value of $(E/N)_{max}$ at which $w(E/N)$ maximizes with the percentage (by number density) of C_2F_4 in Ar.

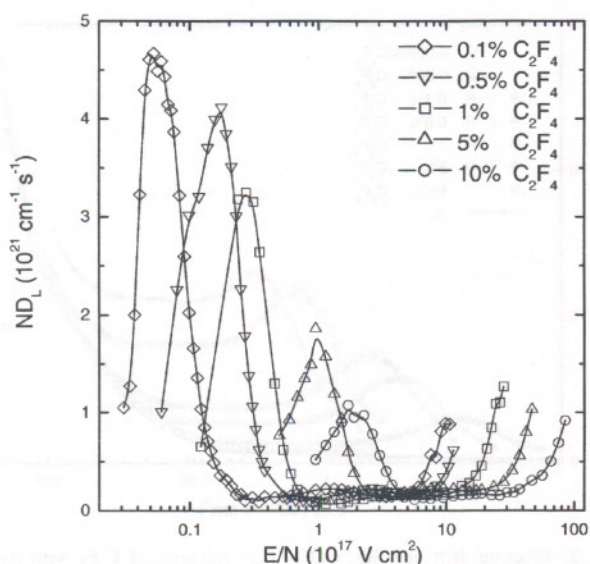


FIG. 4. Density-normalized longitudinal electron diffusion coefficient, ND_L , as a function of E/N for 0.1%, 0.5%, 1%, 5%, and 10% mixtures of C₂F₄ with Ar.

sents values taken from the literature as reported by Dutton.²⁶ Values obtained from least squares fits to the data for each mixture in Fig. 6 are given in Table I.

Interestingly, the measurements in Fig. 6 show that for the low-concentration mixtures, $(\alpha - \eta)/N > 0$ for values of E/N well below the $(E/N)_{lim}$ of Ar. To our knowledge, this is the first time where the $(E/N)_{lim}$ value for a rare gas/molecular gas mixture is found to decrease rather than to increase compared to that for the pure rare gas. To further explore this finding we have plotted the α/N for 100% Ar and for the low concentration ($\leq 1\%$) C₂F₄/Ar mixtures on an expanded linear scale in Fig. 7. This allows a better comparison of the $(\alpha - \eta)/N$ values in the vicinity of $(E/N)_{lim}$. Interestingly, in the E/N region covered by the data in Fig. 7, not only do the values of $(\alpha - \eta)/N$ for the low-

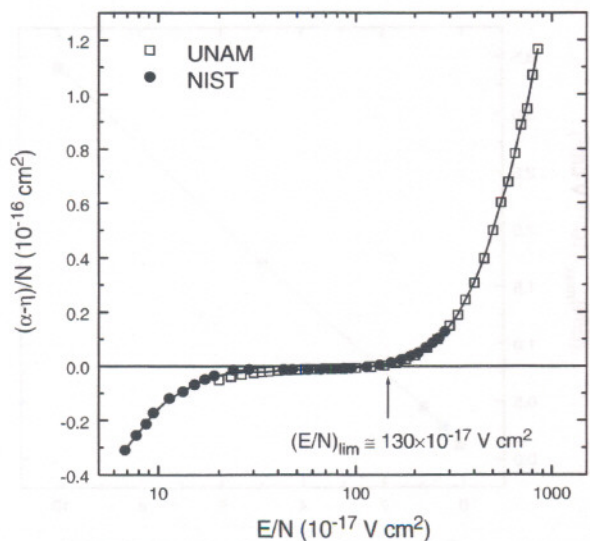


FIG. 5. Density-reduced effective ionization coefficient $(\alpha - \eta)/N$, as a function of E/N for 100% C₂F₄. ●, measurement at NIST; □, measurements at UNAM.

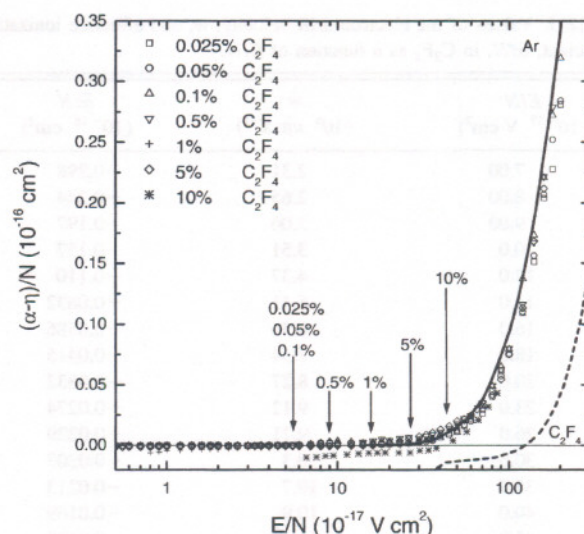


FIG. 6. Density-reduced effective ionization coefficient $(\alpha - \eta)/N$, as a function of E/N for C₂F₄/Ar gas mixtures. *, measurements at NIST; all other measurements were taken at UNAM. The vertical arrows shown in the figure give the locations of the $(E/N)_{lim}$ for each mixture.

concentration C₂F₄/Ar mixtures exceed those for pure Ar, but the observed enhancement in $(\alpha - \eta)/N$ varies with mixture composition and E/N . Where does this extra ionization come from and why does it display the observed characteristics?

An answer to these questions can be advanced by observing that the addition of C₂F₄ to Ar has two opposite effects on $(\alpha - \eta)/N$, and hence on $(E/N)_{lim}$. First, due to enhanced electron scattering by the molecular gas, the electron energy distribution function in the mixture lies at lower electron energies compared to that of 100% Ar. This decrease $(\alpha - \eta)/N$ and increases $(E/N)_{lim}$, as is indeed observed to be the case here for the high concentration C₂F₄/Ar mixtures (5% and 10%), and also for 100% C₂F₄ (see Fig. 6). Second, the low ionization threshold energy of C₂F₄ allows

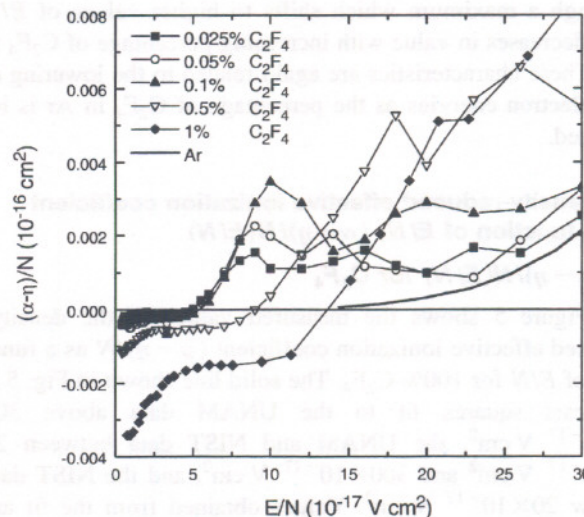


FIG. 7. Density-reduced effective ionization coefficient $(\alpha - \eta)/N$, as a function of E/N for the 0.025% (■), 0.05% (○), 0.1% (▲), 0.5% (▽), and 1% (◆) C₂F₄/Ar gas mixtures shown on an expanded linear E/N scale. For comparison, (α/N) for pure Ar is also shown in the figure (solid line).

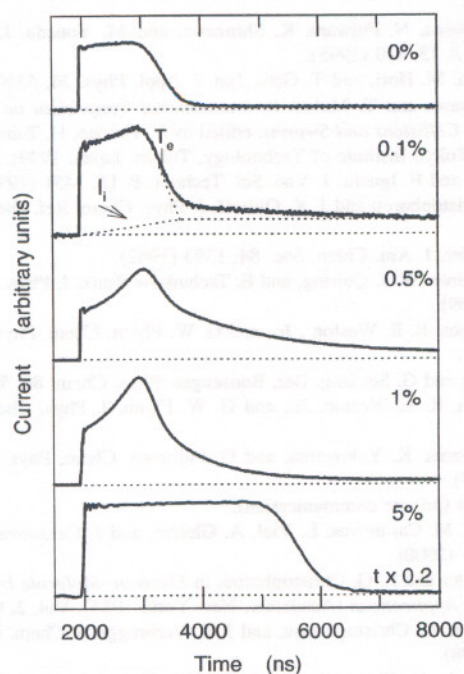
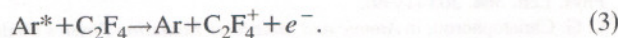


FIG. 8. Electron current waveforms obtained in C_2F_4/Ar mixtures for C_2F_4 concentrations varying from 0% to 5% C_2F_4 for $E/N=26 \times 10^{17} \text{ V cm}^{-2}$. The total gas pressure in all cases is 1.47 kPa (11 Torr). For clarity, the electron transit time (T_e) and the ionic current contribution (I_i) are indicated. Increased ionization as evidenced by the initial rise of the current prior to T_e and delayed ionization as evidenced by the long tail in the current waveform following T_e appear in dilute C_2F_4/Ar mixtures (<5% C_2F_4) from indirect Penning ionization. As the concentration of C_2F_4 reaches 5%, the degree of ionization decreases and the long tail disappears, indicating that the relative significance of Penning ionization lessens in comparison to the more dilute mixtures.

increased free electron production via Penning ionization. C_2F_4 has a much lower ionization threshold energy ($10.12 \pm 0.02 \text{ eV}$ in Ref. 27) than that of Ar (15.8 eV), and thus ionization of C_2F_4 can occur either via direct ionization or by indirect Penning ionization,



This is due to the fact that the ionization threshold energy lies below the set of Ar metastable levels near 11.6 eV. The Penning ionization process (3) has long been shown to substantially increase the total ionization produced in mixtures of rare gases with small concentrations of certain molecular additives. The enhancement in ionization due to this process can be seen in the electron current waveforms shown in Fig. 8 for varying C_2F_4/Ar mixtures at constant E/N and total gas pressure. As can be seen in Fig. 8, the degree of ionization increases as the C_2F_4 concentration in the mixture increases from 0% to 1%. Furthermore, the enhanced ionization is accompanied by the appearance of a long tail in the current waveform due to delayed ionization resulting from Penning ionization processes. As the concentration of C_2F_4 reaches 5%, the degree of ionization decreases and the long tail disappears, indicating that the relative significance of these two effects is reversed. This observation is consistent with earlier reports of increased ionization in Ar mixtures with other dilute molecular additives [see Figs. 2.3 and 2.4(a) in Ref. 28].

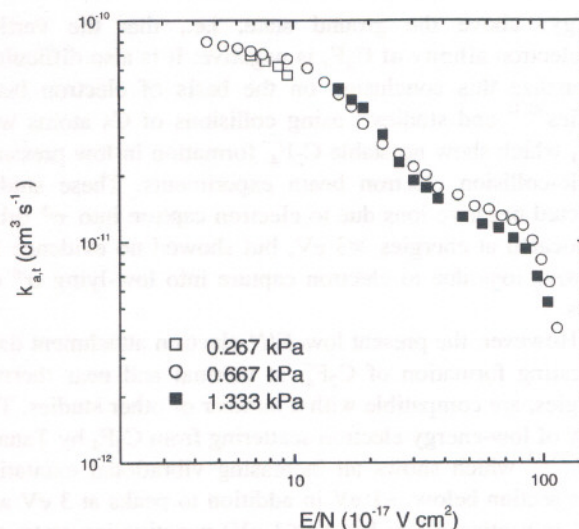


FIG. 9. Total electron attachment rate constant $k_{a,t}$ as a function of E/N for pure C_2F_4 obtained at total pressures of 0.267 kPa (2 Torr), 0.667 kPa (5 Torr), and 1.333 kPa (10 Torr).

The measurements in Figs. 6 and 7, then, indicate that for the low concentration (<5%) C_2F_4/Ar mixtures of the present work, the effect of process (3) is more significant in determining the magnitude of $(\alpha - \eta)/N$, and thus the value of $(E/N)_{lim}$, compared to that of the change in the electron energy distribution function which results from enhanced electron scattering by the molecular additive. It should be noted that the observed variation of $(E/N)_{lim}$ with the relative amount of C_2F_4 in the C_2F_4/Ar mixture is a good example of the breakdown of Paschen's Law. The law only holds when the physical properties of the gaseous medium are not changing with gas pressure and/or gas composition.

D. Total electron attachment rate constant as a function of E/N , $k_{a,t}(E/N)$

Figure 9 shows the total electron attachment rate constant, $k_{a,t}$ of C_2F_4 measured at room temperature ($\sim 300 \text{ K}$) as a function of E/N in 100% C_2F_4 at total pressures of 0.266 kPa, 0.666 kPa, and 1.333 kPa. These data indicate that the measured $k_{a,t}(E/N)$ is due to two processes, one at low E/N ($> 30 \times 10^{-17} \text{ V cm}^{-2}$). The high- E/N process can be understood as originating from the lowest π^* -negative ion state of C_2F_4 located at $\sim 3.0 \text{ eV}$ (vertical attachment energy, Refs. 29 and 30). At these values of E/N there must be a sufficiently high number of electrons with energies $\geq 3 \text{ eV}$ to reach this state, judging from the fact that there are electrons energetic enough to cause ionization at E/N values $\geq 70 \times 10^{-17} \text{ V cm}^{-2}$ (Fig. 5).

The electron attachment data for low E/N in Fig. 9 indicate the formation of $C_2F_4^-$ at thermal and near thermal energies under the swarm conditions of the present experiments, since formation of fragment negative ions is not energetically possible at these low energies. This, in turn, implies a positive electron affinity for the C_2F_4 molecule. This conclusion is difficult to rationalize on the basis of the results of calculations which show (Refs. 29 and 30) that the lowest π^* negative ion state of C_2F_4 lies $\sim 3 \text{ eV}$ (vertical attachment

energy) above the ground state, i.e., that the vertical π^* -electron affinity of C₂F₄ is negative. It is also difficult to rationalize this conclusion on the basis of electron beam studies^{30,31} and studies³¹ using collisions of Cs atoms with C₂F₄ which show no stable C₂F₄⁻ formation in low pressure, single-collision electron beam experiments. These studies detected negative ions due to electron capture into π^* orbitals located at energies ≥ 3 eV, but showed no evidence for negative ions due to electron capture into low-lying σ^* orbitals.

However, the present low-*E/N* electron attachment data, indicating formation of C₂F₄⁻ at thermal and near thermal energies, are compatible with a number of other studies. The study of low-energy electron scattering from C₂F₄ by Tanaka *et al.*^{32,33} which shows an increasing vibrational excitation cross section below ~ 1 eV in addition to peaks at 3 eV and 6 eV indicating a low-lying (< 1 eV) negative ion state; the *ab initio* calculation of Paddon-Row *et al.*³⁴ which predicts the adiabatic electron affinity of C₂F₄ to be ~ 0.0 eV; the multiple scattering X_α calculation of Bloor *et al.*³⁵ which gives for the adiabatic electron affinity of C₂F₄ a value of 0.11 eV; and the ESR study of C₂F₄ in solution by McNeil *et al.*^{36,37} which found stable C₂F₄⁻ ions attributed to electron capture into a σ^* orbital of C₂F₄. Furthermore, C₂F₄⁻ ions were observed via the 3-eV negative ion state [and (C₂F₄)₂⁻ at thermal energies] in studies of electron attachment to C₂F₄ clusters,²⁸ and metastable C₂F₄^{-*} ions (autodetachment lifetimes 14 μ s) were detected²⁹ in studies of dissociative electron attachment in tetrafluorosuccinic anhydride (C₄F₄O₃) where the configuration of C₂F₄ in this molecule is different from that of the free C₂F₄ molecule. It may, thus, be possible that the electron attachment observed in the present study at low *E/N* is not due to impurities but rather to C₂F₄⁻ ions formed by electron capture into a σ^* orbital to C₂F₄.

IV. SUMMARY

Measurements of electron transport, ionization, and effective attachment coefficients are reported for C₂F₄. In addition, measurements of the electron drift velocity and the effective ionization coefficient as a function of the density-reduced electric field *E/N* are reported for mixtures of C₂F₄ with Ar. We observe that for the C₂F₄/Ar mixtures, the measured $(\alpha - \eta)/N$ has two components: one due to direct ionization of C₂F₄ and another due to indirect Penning ionization of C₂F₄ from Ar. We also present the rate constant for electron attachment to C₂F₄ and the product of the longitudinal electron diffusion coefficient and total gas number density, ND_L , for C₂F₄/Ar mixtures as functions of *E/N*.

ACKNOWLEDGMENTS

Work partially supported by DGAPA, UNAM, IN 113898. One of the authors (A.N.G.) gratefully acknowledges the support of a National Research Council postdoctoral associateship. Thanks are due to A. Bustos for technical assistance.

¹H. Kimura, K. Shiozawa, K. Kawai, H. Miyatake, and M. Yoneda, *Jpn. J. Appl. Phys.* **34**, 2114 (1995).

- ²T. Maruyama, N. Fujwara, K. Shiozawa, and M. Yoneda, *J. Vac. Sci. Technol. A* **13**, 810 (1995).
- ³K. Miyata, M. Hori, and T. Goto, *Jpn. J. Appl. Phys.* **36**, 5340 (1997).
- ⁴S. Samukawa and T. Mukai, in *International Symposium on Electron-Molecule Collisions and Swarms*, edited by Y. Hatano, H. Tanaka, and N. Kouchi (Tokyo Institute of Technology, Tokyo, Japan, 1999), p. 76.
- ⁵K. Nojiri and E. Iguchi, *J. Vac. Sci. Technol. B* **13**, 1451 (1995).
- ⁶L. G. Christophorou and J. K. Olthoff, *J. Phys. Chem. Ref. Data* (submitted).
- ⁷J. N. Butler, *J. Am. Chem. Soc.* **84**, 1393 (1962).
- ⁸J. M. Simmie, W. J. Quiring, and E. Tschuikow-Roux, *J. Phys. Chem.* **73**, 3830 (1969).
- ⁹J. M. Preses, R. E. Weston, Jr., and G. W. Flynn, *Chem. Phys. Lett.* **46**, 69 (1977).
- ¹⁰M. Quack and G. Seyfang, *Ber. Bunsenges. Phys. Chem.* **86**, 504 (1982).
- ¹¹E. Pochon, R. E. Weston, Jr., and G. W. Flynn, *J. Phys. Chem.* **89**, 86 (1985).
- ¹²A. Yokoyama, K. Yokoyama, and G. Fujisawa, *Chem. Phys. Lett.* **237**, 106 (1995).
- ¹³A. Gleizes (private communication).
- ¹⁴I. Coll, A. M. Casanovas, L. Vial, A. Gleizes, and J. Casanovas, *J. Phys. D* **33**, 221 (2000).
- ¹⁵S. R. Hunter and L. G. Christophorou, in *Electron-Molecule Interactions and Their Applications* (Academic, New York, 1984), Vol. 2, Chap. 3.
- ¹⁶Y. Wang, L. G. Christophorou, and J. K. Verbrugge, *J. Chem. Phys.* **109**, 8304 (1998).
- ¹⁷Y. Wang, L. G. Christophorou, J. K. Olthoff, and J. K. Verbrugge, in *Gaseous Dielectrics VIII*, edited by L. Christophorou and J. Olthoff (Plenum, New York, 1999), p. 39.
- ¹⁸P. G. Datskos, J. G. Carter, and L. G. Christophorou, *J. Appl. Phys.* **71**, 15 (1991).
- ¹⁹J. de Urquijo, I. Alvarez, E. Basurto, and C. Cisneros, *J. Phys. D* **32**, 1646 (1999).
- ²⁰J. de Urquijo, I. Alvarez, and C. Cisneros, *Phys. Rev. E* **60**, 4990 (1999).
- ²¹Certain commercial equipment, instruments, or materials are identified in this paper in order to specify the experimental procedure adequately. Such identification is not intended to imply recommendation or endorsement by the National Institute of Standards and Technology, nor is it intended to imply that the materials or equipment identified are necessarily the best available for the purpose.
- ²²See EPAPS Document No. E-JCPSA6-114-002121 for tabulated values of electron drift velocities and effective ionization coefficients for C₂F₄ and C₂F₄/Ar mixtures. This document may be retrieved via the EPAPS homepage (<http://www.aip.org/pubservs/epaps.html>) or from <ftp.aip.org> in the directory /epaps/. See the EPAPS homepage for more information.
- ²³L. G. Christophorou, in *Atomic and Molecular Radiation Physics* (Wiley-Interscience, New York, 1971), Chap. 4, p. 239.
- ²⁴Y. Wang, L. G. Christophorou, J. K. Olthoff, and J. K. Verbrugge, *Chem. Phys. Lett.* **304**, 303 (1999).
- ²⁵L. G. Christophorou, in *Atomic and Molecular Radiation Physics* (Wiley-Interscience, New York, 1971), p. 283.
- ²⁶J. Dutton, *J. Phys. Chem. Ref. Data* **4**, 577 (1975).
- ²⁷S. G. Lias, J. E. Bartmess, J. F. Liebman, J. L. Holmes, R. D. Levin, and W. G. Mallard, *J. Phys. Chem. Ref. Data, Suppl.* **17**, 1 (1988).
- ²⁸L. G. Christophorou, *Atomic and Molecular Radiation Physics* (Wiley-Interscience, New York, 1971), Chap. 2, pp. 50 and 52.
- ²⁹N. S. Chiu, P. D. Burrow, and K. D. Jordan, *Chem. Phys. Lett.* **68**, 121 (1979).
- ³⁰E. Illenberger, *Chem. Rev.* **92**, 1589 (1992).
- ³¹C. D. Cooper and R. N. Compton, *J. Chem. Phys.* **60**, 2424 (1974).
- ³²H. Tanaka (private communication).
- ³³M. Okamoto, M. Hoshino, Y. Sakamoto, S. Watanabe, M. Kitajima, H. Tanaka, and M. Kimura, in *Proceedings of the International Symposium on Electron-Molecule Collisions and Swarms*, edited by H. Hatano, H. Tanaka, and N. Kouchi (Tokyo Institute of Technology, Tokyo, Japan, 1999), p. 191.
- ³⁴M. N. Paddon-Row, N. G. Rondan, K. N. Houk, and K. D. Jordan, *J. Am. Chem. Soc.* **104**, 1143 (1982).
- ³⁵J. E. Bloor, R. A. Paysen, and R. E. Sherrod, *Chem. Phys. Lett.* **60**, 476 (1979).
- ³⁶R. I. McNeil, M. Shiotani, F. Williams, and M. B. Yim, *Chem. Phys. Lett.* **51**, 433 (1977).
- ³⁷R. I. McNeil, F. Williams, and M. B. Yim, *Chem. Phys. Lett.* **61**, 293 (1979).

